

A field evaluation of a piezo-optical dosimeter for environmental monitoring of nitrogen dioxide†

John D. Wright,^{*a} Eric F. J. Schillinger,^a Fabrice Cazier,^b Habiba Nouali,^b Agnès Mercier^b and Charles Beaugard^c

^aSchool of Physical Sciences, University of Kent, Canterbury, Kent, UK CT2 7NR.

Fax: +44-1227-827758; Tel: +44-1227-823759

^bCentre Commun de Mesures, MREID, Université du Littoral Côte d'Opale, 145 avenue M. Schuman, 59140 Dunkerque, France. E-mail: cazier@univ-littoral.fr;

Tel: +33-328-658254

^cOpal'Air, 1 route du pont de pierre, 59820 Gravelines, France

Received 30th January 2004, Accepted 25th March 2004

First published as an Advance Article on the web 14th April 2004

Measurements of 8-hour time-weighted average NO₂ concentrations are reported at 7 different locations in the region of Dunkirk over 5 consecutive days using PiezoOptic monitoring badges previously calibrated for the range 0–70 ppb together with data from chemiluminescent analysers in 5 sites (4 fixed and one mobile). The latter facilities also provided data on ozone and NO concentrations and meteorological conditions. Daily averages from the two pairs of badges in different types of sampling cover in each site have been compared with data from the chemiluminescent analysers, and found largely to agree within error margins of $\pm 30\%$. Although NO₂ and ozone concentrations were low, rendering detailed discussion impossible, the general features followed expected patterns.

Introduction

Nitrogen dioxide is one of the most widely measured atmospheric pollutants, and a great deal of research has been directed at the development of new monitoring methods using instruments, sensors and diffusive samplers. Although numerous papers have been published on the development and characterisation of nitrogen dioxide sensors based on various principles (*e.g.* phthalocyanine¹ and metal oxide² semiconductor sensors and optical sensors³), no sensor-based system has yet provided the combination of sensitivity, reproducibility and affordability necessary to gain wide acceptance for environmental monitoring applications. The instrumental reference method for NO₂ monitoring adopted by European Directive 99/30/CE⁴ is the chemiluminescence method. A detailed assessment of the ability of this method to measure ambient NO₂ with an accuracy within 15% as requested by the data quality objective of this European Directive has recently been reported.⁵ The capital and running costs of the chemiluminescence method, as well as the size and power requirement of the instrumentation, mean that it is difficult to use this instrument on the wide scale necessary to determine the distribution of NO₂ pollution, across a city for example. Diffusive samplers⁶ have therefore been commonly used in such studies.⁷ These low cost passive sampling devices have been extensively evaluated⁸ and modelled,⁹ but demand relatively expensive laboratory equipment for analysis. Recently artificial neural networks have been used to project the results of the continuous measurements of a network of fixed chemiluminescence instrument monitoring stations into the spatial distribution characterised by a large number of diffusive sampler devices.¹⁰

† Electronic supplementary information (ESI) available: **Fig. ESI 1** Time profiles of the ozone concentrations for the five days (uv instrument data). **Fig. ESI 2** Temperature profiles (site G) for the five days. **Fig. ESI 3** Wind directions (top) and speeds for the five days (site G). In the direction plots, the lengths of the lines indicate the relative times in each direction and the times of day in each direction are shown as numbers. See <http://www.rsc.org/suppdata/em/b4/b401495m/>

Such developments are clearly only possible where the performance characteristics of the cheaper passive sampling devices are properly understood in relation to those of the reference instrumental method.

Recently we have developed a new type of diffusive sampling device which is comparable in cost to conventional diffusive samplers yet gives instant dose readings in the field at low cost without the need for skilled operators. This is based on the PiezoOptic system, which we have described in detail previously.^{11–16} The system consists of a badge (Fig. 1 and 2) that

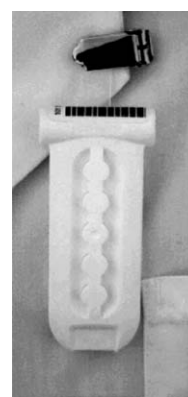


Fig. 1 The PiezoOptic badge.

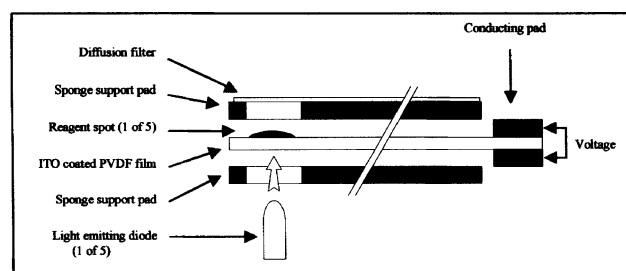


Fig. 2 Schematic diagram of the PiezoOptic badge.



Fig. 3 The PiezOptic badge reader unit.

may be used for many different analytes with appropriate reagents, and a reader unit (Fig. 3) that can be programmed to work for any combination of analyte badges. Five spots of colorimetric reagent are deposited on a polyvinylidene fluoride (PVDF) piezoelectric film coated with a thin optically-transparent conductive layer of indium-tin oxide. The film is supported on both sides by sponge pads in which holes have been die-cut in order to allow both analyte and light to reach the spots. The two sides of the film are contacted at one end by conductive sponge pads. All these components are tightly held inside a polymer casing that gives protection to the reactive spots, allows vapours access to the spots (through a diffusion filter if appropriate), fits inside a slot in the reader and offers apertures for illuminating the spots. When the reagent spot is exposed to the target analyte, a colour change occurs. The quantity of reagent converted to the new colour is directly proportional to the integrated dose (integral of concentration vs. time curve over the standard exposure time) of the target analyte received by the spot. When the exposed spot is illuminated using a light emitting diode (LED) that emits in the wavelength range of the colour change, heat is produced in the spot by non-radiative decay of the excited states. The change in the total heat thus produced is directly proportional to the quantity of reagent that has been converted to the new colour, and hence to the analyte dose. Since heat expands the spot, stressing the underlying PVDF and thus creating a piezoelectric charge which is measured by the reader unit, the change in heat produced is directly reflected in the change in reader output signal. This principle is essentially a form of photoacoustic spectroscopy. To compensate for differences in the light output of different LEDs, and for possible ageing effects, all readings are normalised with reference to the output of a standard screen-printed black PVDF strip exposed before each measurement session.

The application of this system to nitrogen dioxide monitoring was first described in 1998,¹¹ and we have recently reported in more detail on the calibration of an improved version of this badge.¹⁶ In this paper we report the results of a field study in which pairs of these badges were deployed in each of two different sheltering covers in 7 different locations on 5 successive days in the northern French coastal town of Dunkirk. The results were compared with those from fixed monitoring stations using chemiluminescent NO₂ instruments at 4 of the locations, and with a similar instrument in a mobile laboratory at one of the remaining locations on each of the days. These stations also provided data on ozone concentrations to permit correction of the badge readings for the relatively small interference of ozone on the NO₂ readings.¹⁶ One of the stations also provided meteorological data for the region. The objectives of this study were to evaluate the performance of the PiezOptic badges in relation to that of the reference instruments in a pilot-scale study under field conditions, and to obtain data on the spatial and temporal distribution of NO₂ concentrations in this residential and industrial environment in a range of weather conditions in order to test whether the badges are capable of providing representative integrated doses.

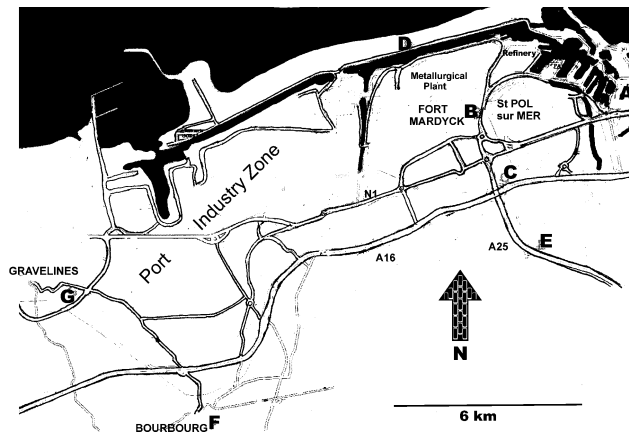


Fig. 4 The location of the sampling sites A-G in Dunkirk.

Dunkirk provides an ideal site for such a study. It has an industrial zone, with a metallurgical plant and a petrochemical refinery, adjacent to a busy commercial port which extends into the residential and shopping centre. To the south, east and west it is well-separated from other cities and pollution sources. It is served by several busy international motorways, representing typical traffic pollution sources. A line drawn from the city to the north extends to the North Pole without intersecting any land. Between the industrial zone and the North Sea lies a long narrow shingle bank surmounted by a motor road. This road is thus expected to be supplied with very clean air when the wind is from the north, but exposed to the full pollution emitted by the industrial zone when the wind is from southerly directions. Finally, the region has a network of pollution and meteorological monitoring stations equipped with (amongst others) chemiluminescent nitrogen oxide and uv ozone monitoring instruments. These stations, operated by OpalAir, provide continuously-logged hourly readings. In this study, readings from 4 of these stations were supplemented by those from a similarly-equipped mobile laboratory operated by the University of Littoral - Opale Coast, and the locations of the 7 monitoring sites selected are shown in Fig. 4. Fig. 5 is a panoramic view of shingle bank site (D) referred to above. The locations of the remaining sites were chosen to give a representative profile of the region. Site A is on a busy city street in the centre of Dunkirk. Site B is in the yard of the fire station in an industrial area close to various refineries, metallurgical plant *etc.* Sites C and G are peri-urban and close to motorways. Sites E and F are further from industrial pollution sources, in rural locations.

Experimental

Approximately 250 PiezOptic badges for NO₂ monitoring, each with two identical reagent spots, were prepared as a single batch and used both for the laboratory calibration reported in reference 16 and for the field studies reported in the present paper. Nitrogen dioxide reagent spots were prepared from a silica sol-gel-entrapped tolidine-based reagent including a



Fig. 5 Panoramic view of site D.



Fig. 6 Badges in the two types of sampling cover.

coupling-enhancer (5-methyl-resorcinol) and humectant (calcium chloride) to obtain the enhanced sensitivity required for the low environmental concentrations to be detected. Tetramethoxysilane (1.38 ml), ethanol (1.5 ml), tolidine (0.4 ml of a saturated solution prepared by stirring 1.28 g with 20 ml ethanol), 5-methyl-resorcinol (0.25 g in 0.5 g ethanol), calcium chloride (0.22 ml of a solution of 4 g in 50 ml water), HCl (0.4 ml of a solution of 5 ml conc. HCl in 200 ml water) and water (0.5 ml) were stirred for 3 minutes and allowed to stand at 35 °C for 24 h. Two separate batches were prepared and combined to provide sufficient material for the entire calibration and measurement programme planned. 0.75 g of the product was then ground in a Retsch MM200 ball mill for 10 min at 25 Hz. Reagent spots were deposited on PVDF strips using 5 µl of a solution of 80 mg of this reagent in 0.5 ml of a solution of 25 mg ml⁻¹ of polyisobutylene in a 3 : 1 toluene-hexane mixture. The badges were packed in pairs in sealed metallised bags and stored in a freezer at -18 °C. These bags were allowed to equilibrate to room temperature for at least 30 minutes before opening prior to deploying the badges.

Two pairs of badges were exposed at each site on each day

for 8 hours. These badges were mounted in the two different types of badge holder shown in Fig. 6. One of these was a simple cover fabricated from a section of plastic domestic guttering fitted with four transverse metal rods providing an open shelf for the two badges. The other was an inverted plastic water bottle with the neck cut off, containing a transverse wire from which the two badges could be suspended inside the bottle. These bottles were covered with aluminium foil to exclude light. The purpose of using these two types of holder was to explore possible effects of different degrees of exposure of the badges to wind, rain and bright light. At the beginning and end of each exposure period the badges were read by the reader unit, which was calibrated using a screen-printed black reference strip at the beginning of each day and, for the first day only, before each set of readings at a given location. (No differences were observed in the data scatter for the first day and subsequent days, so it may safely be concluded that any errors associated with the calibration procedure or drift in the outputs of the reader unit LEDs over a measuring period are negligible.) At the sites of the OpalAir monitoring stations, the badge holders were mounted together on the roof, close to the air intake for the chemiluminescent instrument (Environnement S.A., model AC31M), and at the other sites they were mounted as shown in Fig. 6 in locations close to the mobile laboratory parking site but well removed from the portable generator power supply. Humidity and temperature readings were recorded at the same time as the badge readings, using a Rotronic Hygropalm humidity meter.

For each spot, the change in reader signal over the exposure period was calculated, and averages were produced for each badge. These were corrected for the effect of ozone on the spots, using the time-weighted average ozone readings for the relevant site (or the daily overall average ozone concentration where local data were not available) from the uv ozone analyser instruments (Environnement S.A., model O₃41) in OpalAir stations and the mobile laboratory, with laboratory data¹⁶ for ozone interference in 50%RH conditions. Although the humidity was generally higher than 50% the correction is small as shown in reference 16, and errors from this source are thus very small. The corrected data were converted to NO₂ concentrations using the calibration obtained in reference 16 in 50%RH conditions, since these experiments showed no significant effect on the calibration curve when selected points were remeasured in 70%RH.

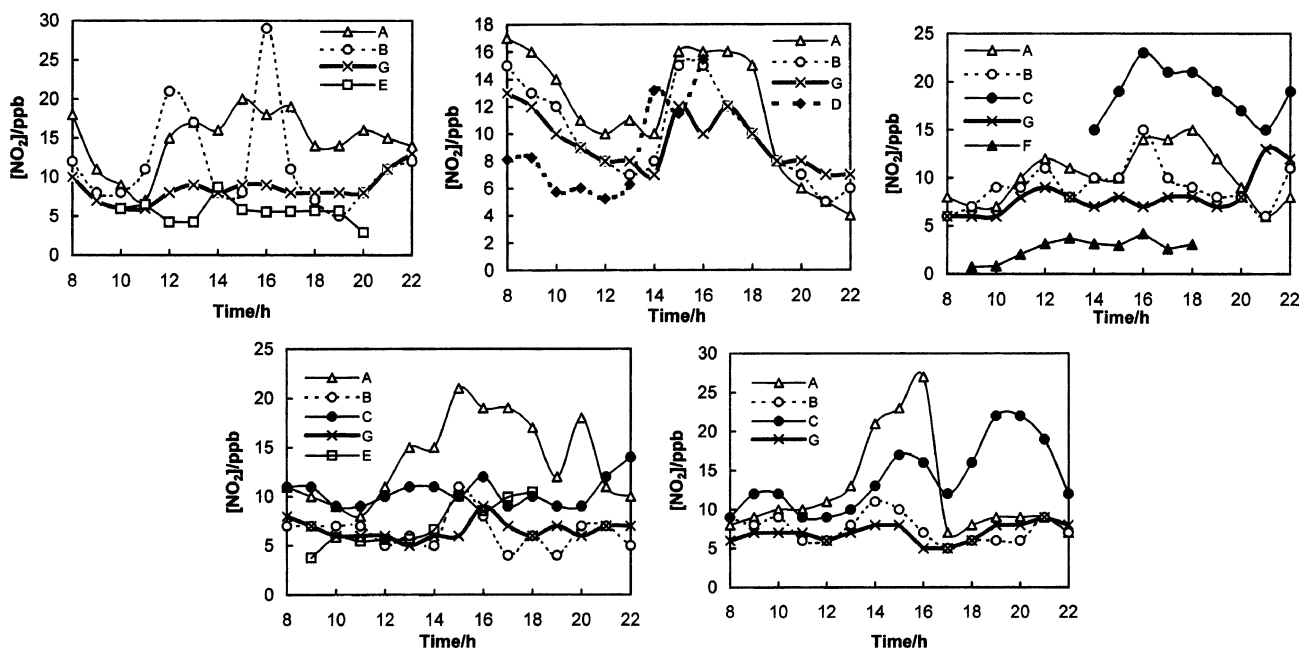


Fig. 7 Time profiles of the NO₂ concentrations for the five days (chemiluminescent instrument data).

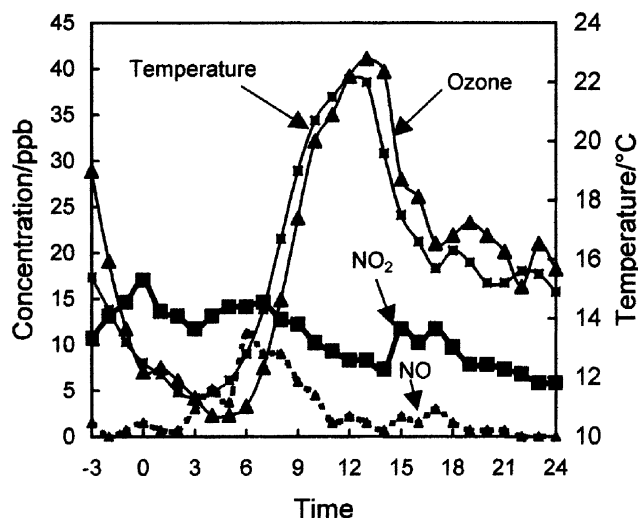


Fig. 8 Concentration and temperature profiles at site G for Tuesday.

Results and discussion

Time profiles of NO₂ were available from the monitoring stations, and these data are shown in Fig. 7. Ozone concentration profiles were similar at all sites, and are available, together with temperature profiles and data on wind speeds and directions, as electronic supplementary information.[†] A typical combined profile of NO₂, NO and ozone concentrations and temperature is shown in Fig. 8. Table 1 shows the complete concentration, temperature and humidity data, and Table 2 summarises the weather conditions during the measurement

campaign. (Note that due to equipment failure, no data were available from the chemiluminescent instrument at site C for the first three days, nor from the mobile laboratory on the final day.)

Fig. 9 shows the correlations between the readings of the two spots on single badges, and between the averages of these two spots for the two badges in each pair. Error bars in both cases are ± 19000 counts (twice the rms deviation of the laboratory calibration points from the fitted curve). The scatter on the former plot is clearly less than on the latter, as reflected in the R^2 values even after exclusion of the worst outliers, and represents effects of non-uniformity in the suspension of ground sol-gel-encapsulated reagent in polymer solution and/or inaccurate placement of the 5 μ l spot on the PVDF strip. The additional scatter on the plot comparing the two badges in each pair must therefore be due to variations in the electrical conductivity of the ITO coating of the PVDF strips or of the contact achieved between the conducting foam pads and the contact pins of the reader. Such effects are likely to be particularly influenced by

Table 2 Summary of weather conditions

Day	Weather conditions
Monday	Sunny all day
Tuesday	Morning: sunny; More and more cloudy in afternoon, heavy rain 16:00–16:30
Wednesday	Morning fine, almost sunny; afternoon wet, heavy rain 12:00–13:45 & 17:00–18:00
Thursday	No heavy rain. Showers at times. Cloudy. Very windy.
Friday	Morning foggy, humid and windy; afternoon sunny and clear

Table 1 Complete experimental data

Day	Site	NO ₂ inst. (ppb)	NO ₂ badge (ppb)	NO (ppb)	O ₃ (ppb)	Temp./°C	%RH	[NO] : [NO ₂]
Monday	A	16.4	20.6	10	32	19.4–20.3	47–48	0.62
	B	13.0	15.5	8	30	17.1–20.9	61–52	0.62
	C	—	12.1	—	39	21.4–18.0	45–59	
	D	—	17.4	—	—	21.4–18.2	51–66	
	E	5.8	10.8	3.1	23.5	17.9–17.6	62–62	0.53
	F	—	12.3	—	—	19.8–18.1	54–60	
	G	8.0	9.4	2	38	17.8–21.2	62–56	0.25
Tuesday	A	12.0	10.3	4	29	17.7-r	68-r	0.31
	B	11.0	21.5(2) ^a	3	30	17.6–18.9	65–71	0.27
	C	—	14.7	—	29	17.7-r	67-r	
	D	8.4	7.4	5.3	36.4	19.2-r	60-r	0.63
	E	—	1.5	—	—	21.7-r	50-r	
	F	—	9.2	—	—	22.1-r	47-r	
	G	9.4	11.5	2	31	21.6-r	51-r	0.22
Wednesday	A	10.5	6.4	5	13	15.5-r	81-r	0.45
	B	9.8	2.8	5	15	16.4-r	77-r	0.50
	C	—	4.2	19	11	16.8–19.4	77–78	0.95
	D	—	4.1(3) ^a	—	—	17.3–17.1	69–80	
	E	—	—	—	—	16.5–19.2	74–84	
	F	2.8	4.7(2) ^a	4.8	17.9	17.9–18.2	69–73	1.70
	G	7.6	8.4(2) ^a	4	18	16.7–18.5	74–77	0.57
Thursday	A	15.5	13.4	12	25	17.7–17.9	73–74	0.67
	B	6.3	8.4	4	30	17.6–16.9	74–74	0.30
	C	9.9	8.7	3	30	18.2-r	79-r	
	D	—	9.0	—	—	16.4–18.0	79–75	
	E	7.2	13.4	5.6	28.6	16.4–18.7	79–68	0.78
	F	—	7.3	—	—	16.8-r	81-r	
	G	6.5	9.7	1	30	17.8–19.3	75–68	0.14
Friday	A	13.9	9.3	16	22	15.0–22.7	78–46	1.14
	B	7.6	7.3	4	24	15.1–22.4	81–45	0.50
	C	13.4	2.5(3) ^a	6	25	14.9–20.2	78–51	0.46
	D	—	8.4	—	—	15.9–17.1	75–71	
	E	—	10.0	—	—	16.2–17.5	69–65	
	F	—	7.5	—	—	15.8–18.9	73–54	
	G	6.8	6.8	1	29	15.4–20.3	75–57	0.14

^a Denotes data from the reduced number of badges indicated due to badge failure. Temperature and humidity data are readings at the beginning and end of each exposure period, and were not recorded during periods of rain, denoted by “r”.

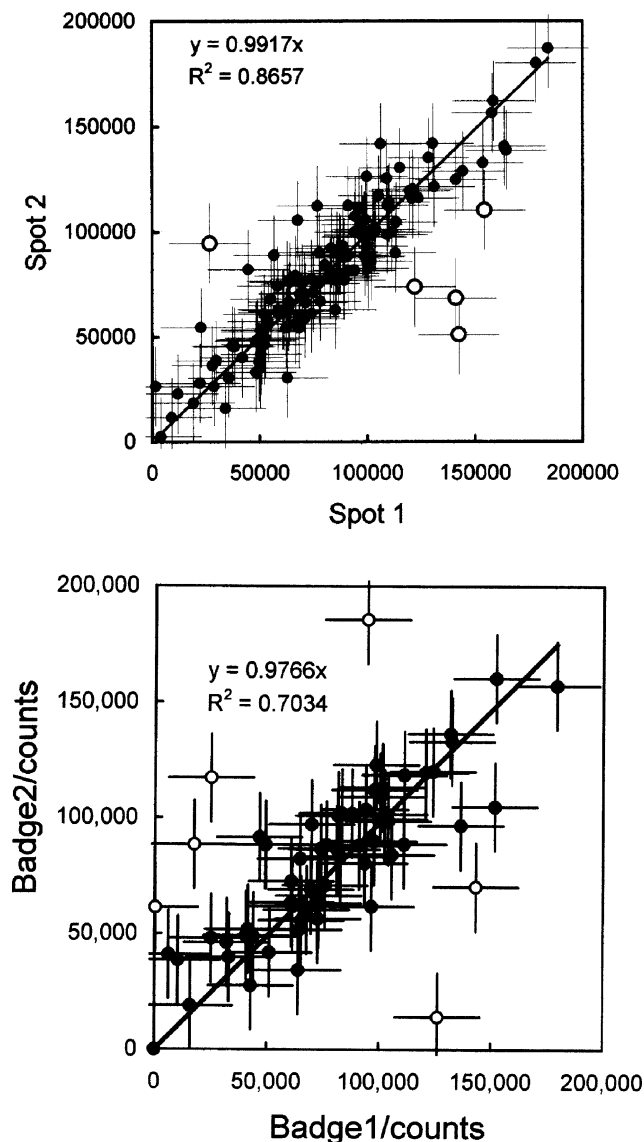


Fig. 9 Comparisons of readings of the two spots on a single badge (top) and the two badges in each type of cover (bottom). The lines are least-squares fits, through the origin, to the points shown as filled circles.

moisture from rain or condensation. These conditions were encountered particularly on Tuesday, Wednesday and Thursday (Table 1) and these were the days on which all of the worst outlier points in this figure (shown as open circles) were recorded. The slopes and R^2 values were therefore calculated omitting these few outliers, with intercepts constrained to zero.

Fig. 10 is a comparison of the averaged badge readings for each of the two types of badge cover. Since the environments of the two pairs of badges are not the same, these data are subject to more variables than in the case of Fig. 9, and experimental quantification of errors arising from these is a major task that cannot be attempted in a study of this scale. We have therefore assumed that the error limits are the same as the relative expanded uncertainty of $\pm 30\%$ recently estimated for the chemiluminescent analyser⁵ or ± 19000 counts, whichever is larger. In fact it is likely that these simple badges have greater uncertainty limits than the instrumental method in field conditions, so these are lower limits and this is confirmed by examination of Fig. 10. No systematic effects can be discerned which might indicate the origins of the scatter. Of the 32 points, there are six most obvious outliers (shown as open circles), of which two occurred on Monday, two on Tuesday and two on Thursday. There are no common features in the temperatures, rain or wind on these days. The three outliers above the line

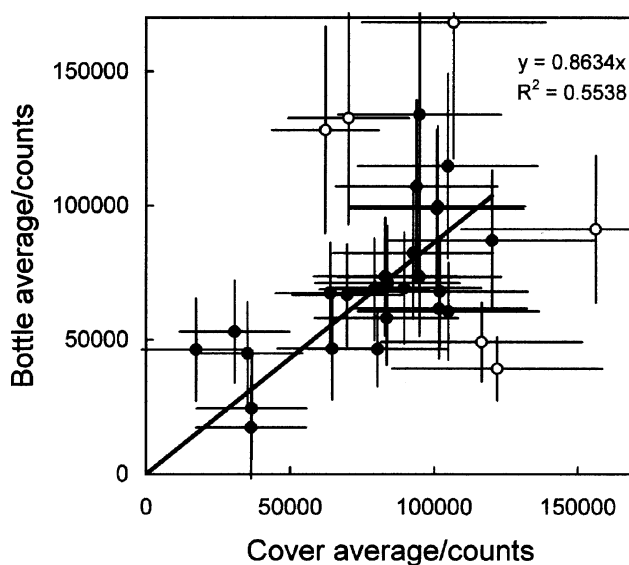


Fig. 10 Comparison of the averaged badge readings (with $\pm 20\%$ error bars) for each of the two types of badge cover. The line is a least-squares fit, through the origin, to the points shown as filled circles.

have spots or badges among the outliers noted in Fig. 9, but the three below the line do not. Unfortunately three of these points were from sites where no instrumental data were available on the relevant days, but for the remaining three the agreements between averaged badge reading and instrument reading were not among the poorest points in Fig. 11 below. We therefore conclude that averaging the values of the 8 spots on 4 badges at each site leads to improved accuracy. This averaging is in fact more extensive than might appear, since the initial and final readings of each spot are both taken during 16 flashes of the LEDs. The first two are discarded as atypical due to effects of the LEDs and circuitry equilibrating after the initialisation of the measurement cycle. The remainder are normalised, the highest and lowest readings are ignored and the remaining 12 readings averaged.

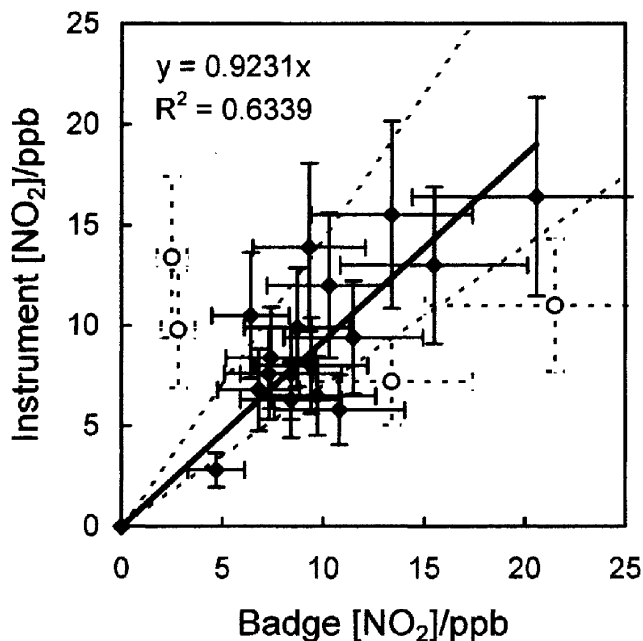


Fig. 11 Comparison of the average NO₂ concentration determined by the badges at each site on a given day with the time-weighted average chemiluminescent instrument data over the same period. Error bars are $\pm 30\%$. The solid line is a least-squares fit, through the origin, to the points shown as filled circles. The two dotted lines represent $\pm 30\%$ deviations from a line of slope 1. Significant outliers are shown as open circles and commented on in the text.

Fig. 11 shows the average readings from the 4 badges at each site, corrected for ozone interference as explained above, plotted against the corresponding chemiluminescent instrument reading. The badge calibration data were fitted to a second-order polynomial curve, and the rms deviation of the experimental points from the fitted curve which was used to derive the concentrations from badge readings was 9596 counts. This is equivalent to 1 ppb. The detection limit and the precision of the badge can both be taken as two standard deviations *i.e.* 2 ppb in laboratory conditions. Since the calibration was done with reference to a simultaneous measurement of the concentration using a reference chemiluminescent analyser, the uncertainty and linearity errors of this analyser (0.8 ppb) are built into the observed rms deviation from the calibration curve, and in laboratory conditions the accuracy can be considered as comparable to the precision. However, in view of the many environmental variables operating, which will affect measurements made using these two very different principles in different ways, it is incorrect to assume that these limits are relevant to the present study. In a recent detailed analysis⁵ Gerboles *et al* concluded that the relative expanded uncertainty of the NO₂ hourly average in field conditions exceeds 30% for NO₂ concentrations less than 20 ppb. They also showed that the major contributors to this uncertainty were the NO concentration and the absolute humidity. The humidity effect was shown to reduce the apparent NO₂ concentration by 0.5% per 1 g m⁻³ of absolute humidity. From the data in Table 2, absolute humidity varied from 8–13.3 g m⁻³ (site A, Monday and site C, Wednesday respectively) during the present study. However, since humidity was not monitored continuously at the instrument sites and it cannot be assumed that the time profiles of NO₂ concentration and humidity are related, it is impossible to make a reliable correction for this effect. Similarly, Table 1 shows that the time weighted average NO concentrations varied by a factor of 19, while the [NO]/[NO₂] ratio ranged from 0.14 to 1.7. Thus, during the measurement period there were significant variations in both the parameters that are most likely to affect the accuracy of the chemiluminescent analyser. Furthermore, five different chemiluminescent analysers were used in the study and no cross-calibration data were available for these within the week of the measurements. Similarly, for the badges, many environmental variables (including temperature, humidity and the presence of other pollutants) could affect the observed response to a given NO₂ concentration. The laboratory calibration was carried out at 50%RH and 20 °C. As mentioned above, no significant effects of humidity were observed during calibration tests. Nevertheless, sudden changes in temperature and humidity led to condensing conditions on several of the sampling days in this study. The effects of liquid films on the badge surfaces could not be characterised in our laboratory calibrations but are expected to be substantial, both in relation to the badge chemical reactions and to the heat transfer processes involved in signal transduction. Temperature changes such as those shown in Fig. 8 represent significant deviations from the calibration temperature of 20 °C. The temperature dependence of the rates of typical colour reactions such as that used here lead to a 15% reduction in response for a 5° temperature decrease. It is not possible to correct for this effect accurately, since the time profiles of NO₂ concentration and temperature are not correlated in a predictable way. Compensation for the effect of ozone interference has already been described in the experimental section, but many other oxidising and reducing pollutants that may be present in this industrial environment could also affect the badge chemical reactions. A much more extensive set of laboratory calibrations, with field measurements of the concentrations of all pollutants having a significant interference effect, would be required to quantify their influences. For all of the above reasons, it is impossible to determine the error limits of the badge readings rigorously.

We have therefore used error bars of $\pm 30\%$ for both axes in Fig. 11 as a basis for discussion of these data. Within these limits, the least-squares best line through the origin has a slope close to 1 and only the four points which have been shown as open circles on the plot fall significantly outside the two broken lines denoting $\pm 30\%$ variation from a line of slope 1. Of these points, two were from sites where badges were noted to be wet (site B, Tuesday and Wednesday), a third (site C, Friday) experienced cool foggy conditions at the start and was noted to give abnormal negative reader signals relative to the normalisation badge, and the fourth (site E, Thursday) has already been noted above as one of the outliers on Fig. 10. It should also be noted that the badges were developed and calibrated to cover a range 0–70 ppb whereas the range actually encountered in this work was 0–20 ppb. Thus the performance of both systems are satisfactory within these uncertainty limits, particularly in view of the varied and often unfavourable weather conditions and the comparatively low NO₂ concentrations encountered.

The low NO₂ concentrations encountered also complicate discussion of concentration variations as a function of location, wind direction and other possible factors. Ozone profiles for different sites on a given day (see Supplementary Information, figure ESI 1†) are more similar than NO₂ profiles, and bear a close relationship to the temperature profiles (Supplementary Information figure ESI 2†) as illustrated in Fig. 8. This suggests that ozone concentrations are mainly determined by solar influx rather than locally generated pollution. Fig. 8 illustrates the effect of the increasing ozone concentration on the nitrogen oxide concentration. The NO₂ concentration falls as the ozone concentration rises, due to photochemical reactions generating a typical photochemical smog, and rises again as the ozone concentration drops. However, correlations of this type are not observed for all sites and days, and additional local pollution sources also influence the nitrogen oxide concentrations, as reflected by the influence of wind direction (see Supplementary Information figure ESI 3†). For example, on Thursday and Friday when the wind was predominantly from the West, the NO₂ pollution from the industrial zone West of Dunkirk was transported towards the city centre (*e.g.* site A) increasing the observed concentrations and away from Gravelines (site G), leading to low concentrations at this site. Conversely, on Tuesday when the wind was predominantly from the East, the NO₂ concentrations at site A were typically about 5 ppb lower than on Thursday and Friday, while those at Gravelines (site G) were typically 5 ppb higher than on those days.

Throughout the studied period, the NO₂ concentrations were low (nearly always below 20 ppb) compared to the values of up to 300 ppb that have been observed in major cities in the worst pollution episodes. This is probably due to the relatively isolated coastal location of Dunkirk, with relatively clean winds diluting pollution from local sources, together with the rainfall washing the NO₂ from the atmosphere on Tuesday, Wednesday and Thursday.

Conclusions

This study has involved a total of 140 PiezOptic badges, each with two identical measuring spots for NO₂, at 7 different sites over 5 days, with simultaneous monitoring by chemiluminescent and other instruments at 5 of the locations on each day. The averages of 12 separate readings of each spot before and after exposure have been used with laboratory calibration data to determine NO₂ concentrations, applying a small correction for ozone interference based on data from uv analyser instruments. Averages from two pairs of badges in different types of sampling cover in each site have been compared with data from the chemiluminescent analysers, and found largely to agree within error margins of $\pm 30\%$. Although NO₂ and ozone concentrations were low, rendering detailed discussion

impossible, the general features followed expected patterns: the ozone concentration profiles followed those of temperature and were similar at all sites. NO₂ concentration profiles showed the influence of photochemical reactions and effects of wind-driven local transport of pollutants. The study shows the value of a data-intensive study of this type, both in understanding local pollution and in evaluating the performance of new methods of pollution monitoring. A much more extensive study, over a longer period with a wider range of pollution levels, is needed to check the conclusions of this preliminary study and to characterise the effects of the many other environmental variables that we are presently unable to quantify. The resources required for such a study are considerable and beyond those available to us in the present work.

Acknowledgements

We thank PiezOptic Ltd., Ashford, Kent for assistance and advice on the use of the PiezOptic system and for providing the badges and reader used in this work. This project was supported by EU Interreg II programme 99/06/C8/06.

References

- (a) J. D. Wright, *Prog. Surf. Sci.*, 1989, **31**, 1; (b) A. V. Chadwick, A. Wilson and J. D. Wright, *Sens. Actuators, B*, 1991, **4**, 499; (c) A. Wilson, G. P. Rigby, J. D. Wright, S. C. Thorpe, T. Terui and Y. Maruyama, *J. Mater. Chem.*, 1992, **2**, 303; (d) P. Roisin, J. D. Wright, R. J. M. Nolte, O. E. Sielcken and S. C. Thorpe, *J. Mater. Chem.*, 1992, **2**, 131.
- (a) N. Yamazoe and N. Miura, in *Gas Sensors*, ed. G. Sverbeglieri, Kluwer, Dordrecht, The Netherlands, 1992, 9–12, 22–24; (b) A. Gurlo, A. Bårsan, M. Ivanovskaya, U. Weimar and W. Göpel, *Sens. Actuators, B*, 1998, **47**, 92.
- (a) B. E. Saltzman, *Anal. Chem.*, 1954, **26**, 1949; (b) J. E. Lambert, E. L. Trump and J. V. Paukstelis, *Environ. Sci. Technol.*, 1987, **21**, 497; (c) *Air Monitoring by Spectroscopic Techniques*, ed. M. W. Sigrist, Wiley, New York, 1994.
- Off. J. Eur. Communities*, 1999, **L163**, 41.
- M. Gerboles, F. Lagler, D. Rembges and C. Brun, *J. Environ. Monit.*, 2003, **5**, 529.
- (a) E. D. Palmes, A. F. Gunnison, J. DiMattio and C. Tomczyk, *Am. Ind. Hyg. Assoc. J.*, 1976, **37**, 570; (b) H. Yanagisawa and H. Nishimura, *Environ. Int.*, 1982, **8**, 235; (c) M. Ferm and P. A. Svanberg, *Atmos. Environ.*, 1998, **8**, 1377.
- (a) A. Fromage-Mariette, S. LeMeur, M. Bobbia, S. Garcia-Fouque, H. Plaisance, J.-L. Houdret and C. Roth, *Proc. Int. Conf. Meas. Air Pollutants by Diffusive Sampling, Montpellier*, 2001, 124; (b) S. Rodriguez and W. Baehler, *Proc. Int. Conf. Meas. Air Pollutants by Diffusive Sampling, Montpellier*, 2001, 133; (c) F. Ferreira, H. Tente, P. Torres, S. Mesquita, E. Santos, F. Esgalhado and D. Jardim, *Proc. Int. Conf. Meas. Air Pollutants by Diffusive Sampling, Montpellier*, 2001, 139.
- (a) H. van Reeuwijk, P. H. Fischer, H. Harssema, D. J. Briggs, K. Smallbone and A. Leuret, *Environ. Monit. Assess.*, 1992, **50**, 37; (b) A. Hagenbjörk-Gustafsson, R. Lindahl, J.-O. Levin and D. Karlsson, *J. Environ. Monit.*, 1999, **1**, 349.
- (a) C. E. Williams, P. N. Pintauro and R. J. Rando, *Am. Ind. Hyg. Assoc. J.*, 1995, **56**, 1074; (b) M. Ferm, *Proc. Int. Conf. Meas. Air Pollutants by Diffusive Sampling, Montpellier*, 2001, 31.
- M. Gerboles, *Proc. Int. Conf. Meas. Air Pollutants by Diffusive Sampling, Montpellier*, 2001, 273.
- F. Colin, P. D. Shepherd, T. J. N. Carter and J. D. Wright, *Sens. Actuators, B*, 1998, **51**, 244.
- J. D. Wright, F. Colin, R. M. Stöckle, P. D. Shepherd, T. Labayen and T. J. N. Carter, *Sens. Actuators, B*, 1998, **51**, 121.
- J. D. Wright, C. von Bültzingslöwen, T. J. N. Carter, F. Colin, P. D. Shepherd, J. V. Oliver, S. J. Holder and R. J. M. Nolte, *J. Mater. Chem.*, 2000, **10**, 175.
- K. R. Bearman, D. C. Blackmore, T. J. N. Carter, F. Colin, S. A. Ross and J. D. Wright, in *Novel Optical Sensors for Industrial and Environmental Monitoring*, ed. R. Narayanaswamy and O. Wolfbeis, Springer, Heidelberg, 2003, ch. 9, p. 203.
- K. R. Bearman, D. C. Blackmore, T. J. N. Carter, F. Colin, J. D. Wright and S. A. Ross, *Chem. Commun.*, 2002, 980.
- E. F. J. Schillinger and J. D. Wright, *Sens. Actuators, B*, 2004, **98**, 262.